17th World Conference on Earthquake Engineering, 17WCEE
Sendai, Japan - September 13th to 18th 2020

GLOBAL OPTIMIZATION OF NUMERICAL TWO-LAYER MODEL USING OBSERVED DATA: A CASE STUDY OF THE 2018 SUNDA STRAITS TSUNAMI

K. Pakoksung[(1)], A. Suppasri[(2)], A. Muhari[(3)], S. Syamsidik[(4)], F. Imamura[(5)]

[(1)] *Postdoctoral Fellow, International Research Institute of Disaster Science, Tohoku University, pakoksung@irides.tohoku.ac.jp*
[(2)] *Associate Professor, International Research Institute of Disaster Science, Tohoku University, suppasri@irides.tohoku.ac.jp*
[(3)] *Head of Coastal Disaster Mitigation Section, Ministry of Marine Affairs and Fisheries, Indonesia, abdul.muhari@kkp.go.id*
[(4)] *Lecturer, Tsunami and Disaster Mitigation Research Center (TDMRC), Universitas Syiah Kuala-Indonesia, syamsidik@tdmrc.org*
[(5)] *Professor, International Research Institute of Disaster Science, Tohoku University, imamura@irides.tohoku.ac.jp*

Abstract

A large landslide occurred on the southwest part of the Anak Krakatoa volcano because of its eruption and generated large tsunami around the Sunda Strait, Indonesia, on 22 December 2018. Upon entering the sea, it caused a huge tsunami that traveled approximately ~5 km across the strait basin and inundated the shore of Sumatra and Java with vertical runup of up to 13 m. Following the event, observed field data, GPS measurements of the inundation and multibeam echo soundings of the straits bathymetry, were collected and provided. Using the provided data set, numerical modeling of the tsunami has been conducted using TUNAMI two-layer model (soil and water) that based on a combination of landslide-source and bathymetry dataset. The two-layer model was implemented to nesting grid system using the finest grid size of 20 m. To constrain unknown landslide parameters, a global optimization algorithm, Differential Evolution, was applied. This resulted in a parameter set that minimized the deviation from measured bathymetry after the event. The global optimization procedure, Differential Evolution (DE), proved to be an effective method to determine the landslide parameters used in the model with the minimum deviation from measured sea bottom. The lowest derivative from measured bathymetry is obtained for best fitting parameter, maximum landslide thickness of 301.2 m and landslide time of 10.8 minutes. The great number of objective function evaluations to locate the minimum with the DE procedure finished it necessary to fix the grid cell size to 20 m. This caused a limitation on the accuracy of the obtained parameter values for the two-layer model. However, the impact landslide time and the thickness, considering generalizations in the modeling of landslide movement, must be carefully calculated to obtain a suitable accuracy.

Keywords: 2018 Sunda Strait tsunami, Subaerial/submarine landslide, Global optimization, Two-later modeling

1. Introduction

A large landslide occurred on the southwest part of the Anak Krakatoa volcano because of its eruption. Landslide generated large tsunami around the Sunda Strait, Indonesia, on 22 December 2018. Upon entering the sea, it caused a huge tsunami that traveled approximately ~5 km across the strait basin and inundated the shore of Sumatra and Java with vertical runup of up to 13 m. [1]. Following the event, observed field data, GPS measurements of the inundation and multibeam echo soundings of the straits bathymetry, were collected and provided [1, 2]. Figure 1 shows a map of the Sunda Straits in addition to the location of the Anak Krakatau in a middle of the straits.

Numerical modeling of submarine or subaerial landslide-generated tsunamis implicates different methods if the conclusions are displayed as completely coupled schemes. The numerical models of coupled dynamic schemes for landslide-generated tsunamis are limited [3, 4], while those for earthquake-generated tsunamis are developed and widely implemented. There have been several studies of landslide-generated tsunamis using nonlinear shallow-water hydrostatic models [5 - 7], Boussinesq nonhydrostatic models [8], the MOST model [9], the COMCOT model [10], and the TUNAMI-N2 model [11]. Moreover, several studies have been performed to model these mechanisms using other uncoupled methods, in which the generation and propagation periods are episodic [12, 13]. One such example is the conceptual model of the BIG'95 submarine landslide and numerical simulation of the propagation of the generated tsunami wave [14 - 18]. In the case of Palu tsunami, the TUNAMI-N2 model is applied to model the submarine landslide tsunami in the Palu Bay [19].

This tsunami event of the Anak Krakatau was recently modeled [20] that the 3D model NHWAVE [21, 22] simulated the landslide and the 2D model FUNWAVE-TVD [23] modeled the tsunami propagation. It was also that the COMCOT model, Cornell Multi-grid Coupled Tsunami Model [10, 24], was used to model this event [25]. The initial sea surface elevation was identified as the landslide source. In this study, the TUNAMI-N2 two-layer [26, 19] model is implemented to model the 2018 Anak Krakatau tsunami.

The point of this study is to investigate the possible source of the 2018 Sunda Straits tsunami using preliminary data. This study focus on the tsunamis generated by subaerial/submarine landslide and the method to find the source is to apply an optimization procedure to determine unknown landslide parameter through comparison between measured and simulated bathymetry in an inverse modeling methodology.

2. Methodology

This paper is supported by four components. First, the hypothesis subaerial/submarine landslide modeling is identified in this study; second, the topography and bathymetry data area used to generate a tsunami model; third, the numerical model is used to reproduce the landslide movement and tsunami propagation; and fourth, the optimization procedure is applied to determine optimal parameters of the landslide.

2.1 Subaerial/submarine landslide modeling

The basic assumption of this study is that the 2018 tsunami in Sunda Straits was initially generated as a subaerial/submarine landslide tsunami by a soil movement of materials originally located on the upper slope. This process produced a subaerial and submarine landslide on the land and seafloor, forming a submarine deposit. The huge slide was probably triggered by the Anak Krakatau volcano eruption. The sunaerail and submarine landslide should have produced a tsunami that affected the coastal area of the Sunda Straits.

The hypothesized landslide locations on the Anak Krakatau are shown in **Fig. 2**, and these landslides can be detected by the satellite image in before and after. The landslides are located in different area of coast line and were the main cause of the studied tsunami. The change of the coast line was used to consider the landslide model, using the 3D ellipsoid modeling.

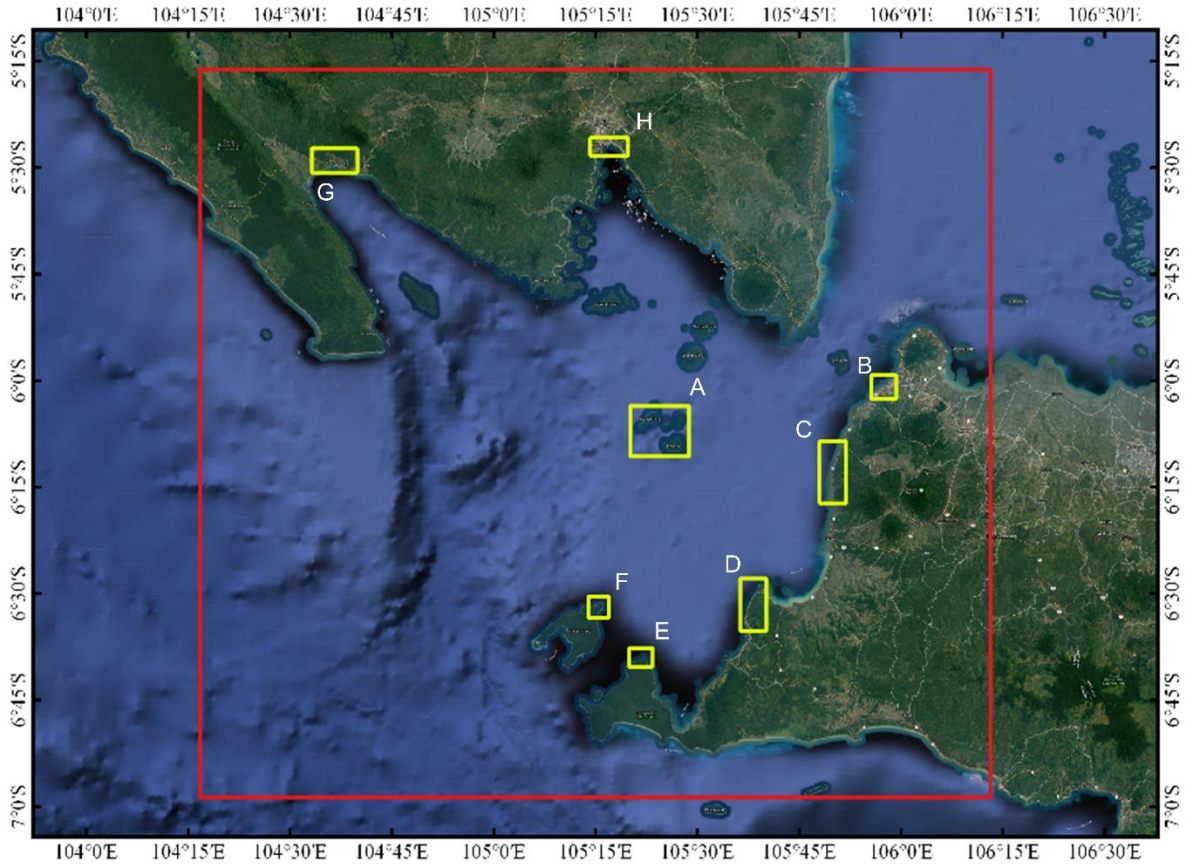

Fig. 1 – Computation domain for tsunami model in Sunda Strait Sea. The red box represents the main region of 180 m resolution and the interested region of 20 m resolution is the yellow box.

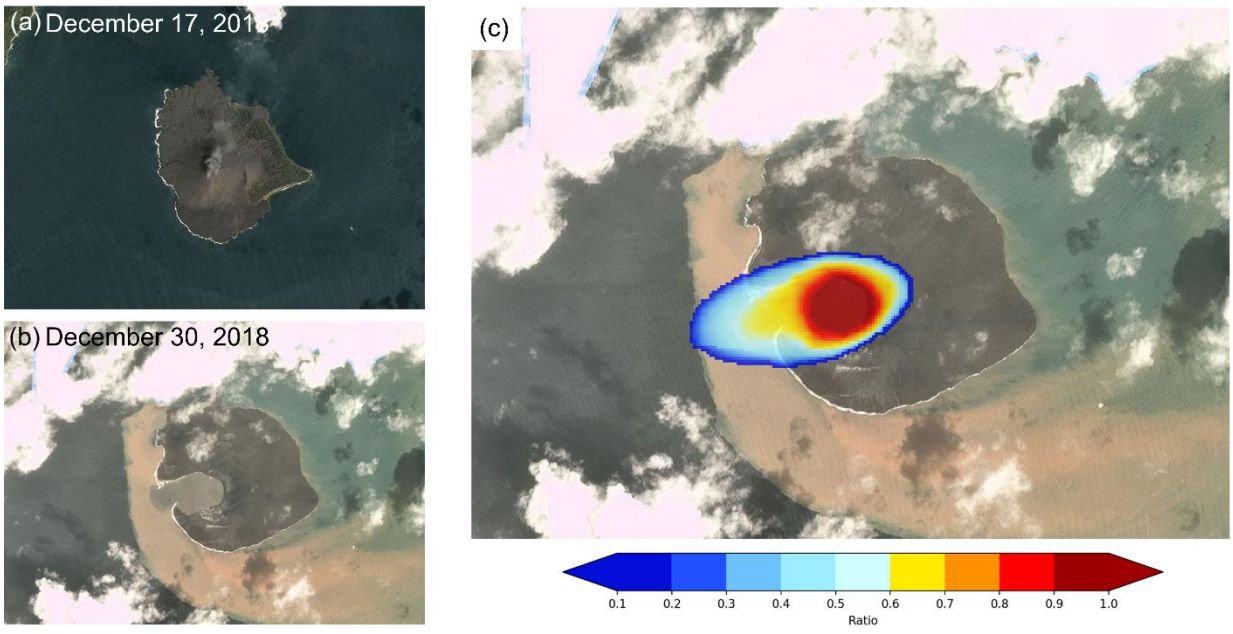

Fig. 2 – Landslide modeling for the 2018 Anak Krakatau eruption, a) satellite image in before, b) satellite image in after, and c) Landslide modeling base on 3D ellipsoid model.

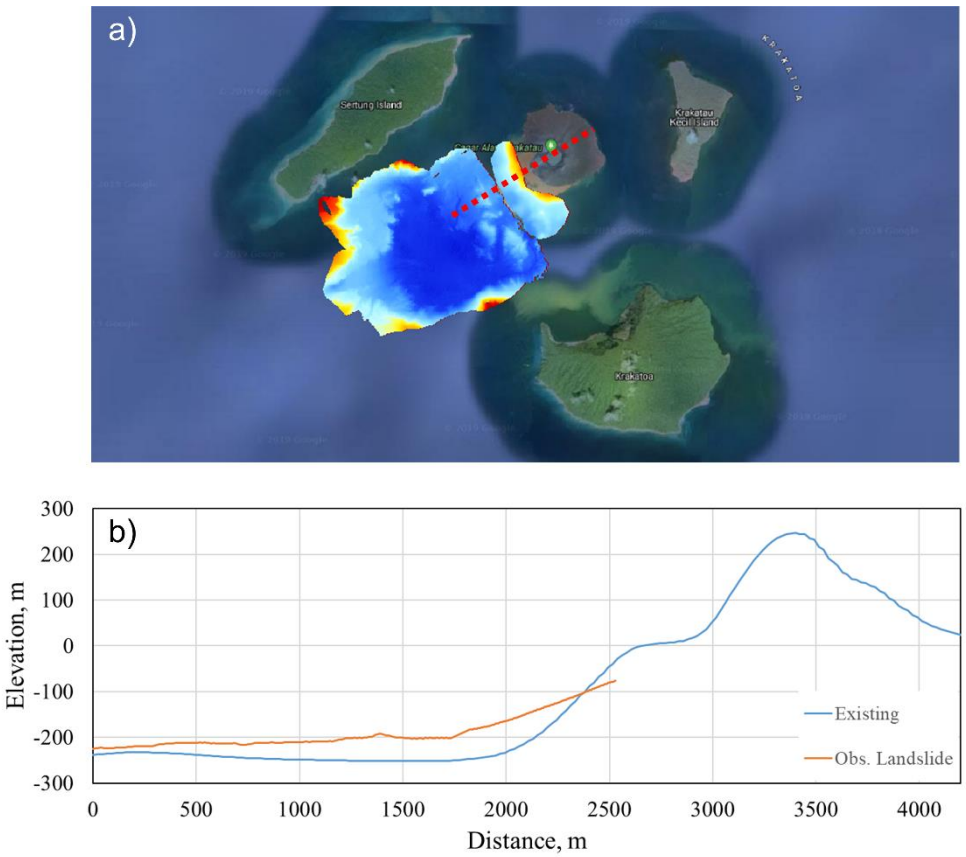

Fig. 3 – Observed bathymetry data after the Anak Krakatau eruption, a) the serveyed area, and b) the comparison between previous and current bathymetry along the red dot line in top panel.

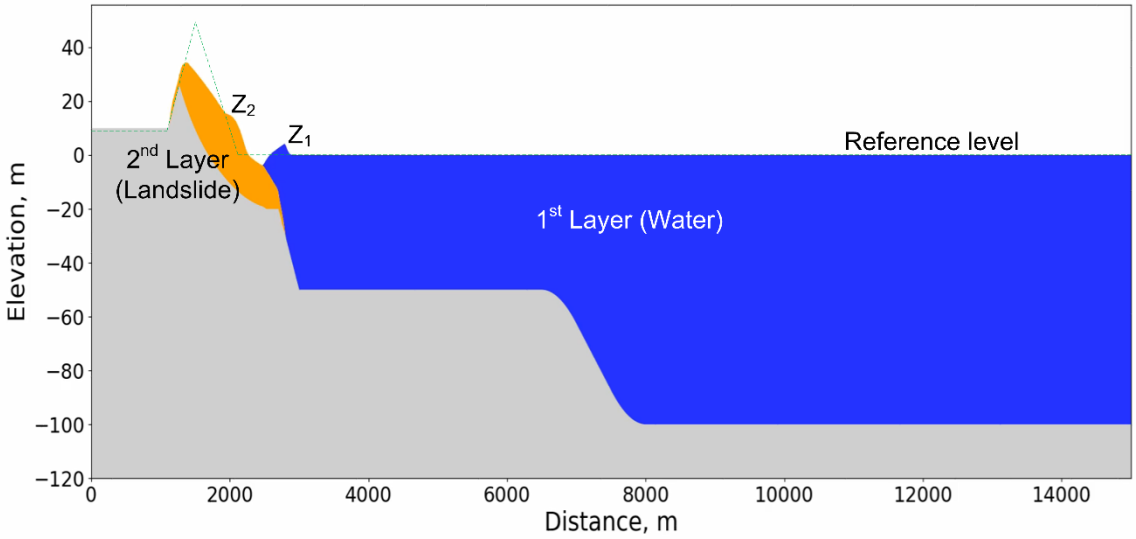

Fig. 4 – Two-layer conceptual schematic of the parameter for modeling the subaerial/submarine landslide.

2.2 Topography and bathymetry data

The complete bathymetric and topographic data from throughout Sunda Straits and surrounding continental areas were provided by BIG. The data consist of two datasets with 180 m resolution for the bathymetry in the sea and 8 m resolution for the topography on land. Both datasets were resampled to 2 domains resolution, 180 m and 20 m (study area in **Fig. 1**). The 180 m resolution domain was resulted in 1079 columns and 956 rows covering the Sunda Straits area.

The Naval Hydrographic and Oceanographic Center of Indonesia used multibeam sonar equipment to survey bathymetry after the Anak Krakatau eruption [1]. The measured area of the new bathymetry covered only the front of the volcano collapse caldera, as shows in **Fig. 3**.

2.3 Numerical model

The tsunami model in the Sunda Straits was assessed with a two-layer numerical model that was developed to solve nonlinear shallow-water equations with two interfacing layers and appropriate kinematic and dynamic boundary conditions at the land and seafloor, interface, and water surface [26, 19]. This two-layer numerical model simulates landslide-generated tsunamis by modeling the interactions between tsunami generation and subaerial/submarine landslides as upper and lower layers. Subaerail/submarine landslides produce tsunami waves similar to those from earthquakes, with a vertical displacement of the seafloor creating a similar displacement at the sea surface, as shown in **Fig. 4**. The mathematical model applied in the landslide–tsunami code is collected of a stratified medium with two layers, as shown in **Fig. 4**. The first layer is composed of a homogeneous inviscid fluid with constant density ρ_1 representing seawater, and the second layer is based on a fluidized granular material with density ρ_s and porosity φ. In this study, the mean density of the fluidized debris is constant and equals $\rho_2 = (1-\varphi)\rho_s + \varphi\rho_1$, as noted in previous research [27]. The two fluids, water and fluidized debris, are hypothesized to be immiscible in this study. The governing equations are written as follows:

Continuity equation of the 1st layer.

$$\frac{\partial Z_1}{\partial t} + \frac{\partial Q_{1x}}{\partial x} + \frac{\partial Q_{1y}}{\partial y} = 0$$

Momentum equations of the 1st layer in the X and Y directions.

$$\frac{\partial Q_{1x}}{\partial t} + \frac{\partial}{\partial x}\left(\frac{Q_{1x}^2}{D_1}\right) + \frac{\partial}{\partial y}\left(\frac{Q_{1x}Q_{1y}}{D_1}\right) + gD_1\frac{\partial Z_1}{\partial x} + gD_1\frac{\partial Z_2}{\partial x} + \tau_{1x} = 0$$

$$\frac{\partial Q_{1y}}{\partial t} + \frac{\partial}{\partial x}\left(\frac{Q_{1x}Q_{1y}}{D_1}\right) + \frac{\partial}{\partial y}\left(\frac{Q_{1y}^2}{D_1}\right) + gD_1\frac{\partial Z_1}{\partial y} + gD_1\frac{\partial Z_2}{\partial y} + \tau_{1y} = 0$$

Continuity equation of the 2nd layer.

$$\frac{\partial Z_2}{\partial t} + \frac{\partial Q_{2x}}{\partial x} + \frac{\partial Q_{2y}}{\partial y} = 0$$

Momentum equations of the 2nd layer in the X and Y directions.

$$\frac{\partial Q_{2x}}{\partial t} + \frac{\partial}{\partial x}\left(\frac{Q_{2x}^2}{D_2}\right) + \frac{\partial}{\partial y}\left(\frac{Q_{2x}Q_{2y}}{D_2}\right) + gD_2\frac{\partial Z_2}{\partial x} + gD_2\frac{\rho_1}{\rho_2}\frac{\partial Z_1}{\partial x} + \tau_{2x} = 0$$

$$\frac{\partial Q_{2y}}{\partial t} + \frac{\partial}{\partial x}\left(\frac{Q_{2x}Q_{2y}}{D_2}\right) + \frac{\partial}{\partial y}\left(\frac{Q_{2y}^2}{D_2}\right) + gD_2\frac{\partial Z_2}{\partial y} + gD_2\frac{\rho_1}{\rho_2}\frac{\partial Z_1}{\partial y} + \tau_{2y} = 0 \quad (1)$$

where index 1 relates to the upper layer and index 2 indicates the second layer. $Z_i(x,y,t)$, $i = 1,2$ is the level of the layer at each point (x,y) at time t, where the level value is measured from a given reference level. $Q_i(x,y,t)$, $i = 1,2$ is the vertically integrated discharge in the x and y directions. g is the gravitational acceleration, and ρ_1 and ρ_2 are the densities of the 1st layer and 2nd layer, respectively. $\tau_i(x,y,t)$ is the bottom

stress in each layer at each point (x, y) at time t. In system 1, the interaction between the 1st layer and the 2nd layer is determined by the fifth term of the momentum equation.

2.4 Landslide parameter sensitivity and optimization

Based on the uncertainty characteristic in the parameter of landslide movement, an inverse method was applied to determine optimal parameters that suitably describe the bathymetry after the volcano eruption. For the two-layer model, the best-fit parameters were estimated by a grid search whereby different combinations of parameters repeatedly run on the model. A set of initial models were approached to obtain a rough idea of landslide parameter ranges. Two parameters were varied that the maximum landslide depth and the sliding time od landslide. The objective function, quality of fit, was considered by the sum square error (SE) index as a summation of squared differences between observed and simulated bathymetry at the spatial in front of the volcano.

$$SE = \sum_{i=1}^{n} \left(y_i^{(obs.)} - y_i^{(sim.)} \right)^2 \tag{2}$$

The grid search method initializes that the result of the sum square error in a spare of a parameter is complex with a gradient-based minimization process, was unsuccessful to get stuck in a local minimum. Then, a global optimization procedure was selected to test the parameter space. The Differential Evolution (DE) procedure as provided by Storn and Price [28], was selected and implemented to the Eq. (1), as show the stream line in **Fig.5**. DE is a simple method and uses a few control variables to control the minimization. The method has a good performance to compare to other minimization procedure, based on a test dataset. On a stochastic search method, it is started from the random generation of parameter vectors, and new trial vectors are determined by disturbing a target vector from the existing vectors. The two-layer model is run by the trial vector parameters if its result of the objective function is lower than the trial vector replaces the target vector [29].

3. Results

Numerical tsunami simulation results from possible subaerial/submarine landslide sources are presented in this section. The original position and final position areas were investigated to assess the impact of a tsunami generated by a volcanic landslide. The level of the potential tsunami on the coastal area was investigated on the basis of the maximum tsunami amplitude at the shoreline and coastal area, defined as the maximum tsunami height from the possible submarine landslide scenario. The maximum tsunami amplitude and inundation area from numerical modeling were calculated from terrain data with a grid size of 20 m for a simulation time of 90 minutes.

Using the Two-layer model, the landslide of the Anak Krakatau eruption was simulated for a range of values of each parameter to get rough boundary on the values which best fit the observed bathymetry. The parameters that were varied were the maximum landslide depth in the range 100 – 450 m and the slideing time in the range 1 – 20 minutes. Other parameters were kept fixed at water density = 1000 kg/m3, landslide density = 2,000 kg/m3, and manning coefficient = 0.025.

The global optimization method using Differential Evolution in section 2.4 was applied to determine the optimal landslide parameters. For the maximum thickness (D) and sliding time (T), the optimization was run with the bounds $100 \leq D \leq 450$ m and $1 \leq T \leq 20$ minutes, as results are shown in **Fig. 6a**. The lowest deviation from measured bathymetry is obtained for the parameter ranges $250 \leq D \leq 400$ m and $7.5 \leq T \leq 13.5$ minutes. The Two-layer model calculated soil movement for a landslide model with parameters in the best fitting range, D = 301.2 m and T = 10.8 minutes is shown in **Fig. 6b** along with the section line in **Fig. 3a**. Overall, the fit is very good and improvement for the underwater area is far from the shore approximately 1 km.

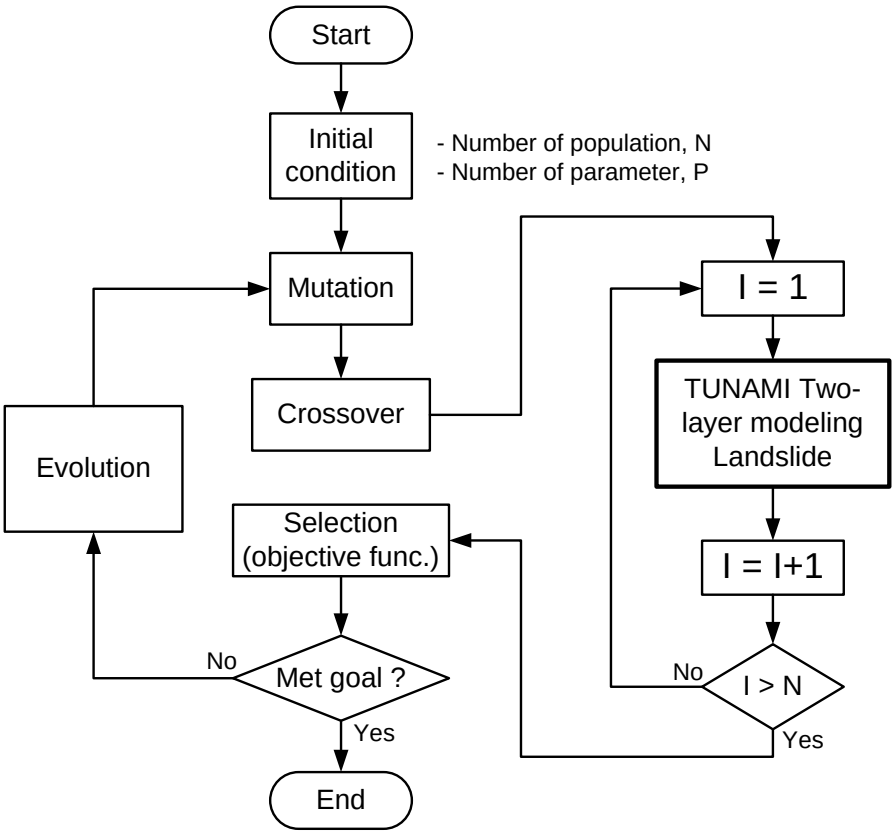

Fig. 5 – Stream line of global optimization combined to Two-layer model for modeling the subaerial/submarine landslide.

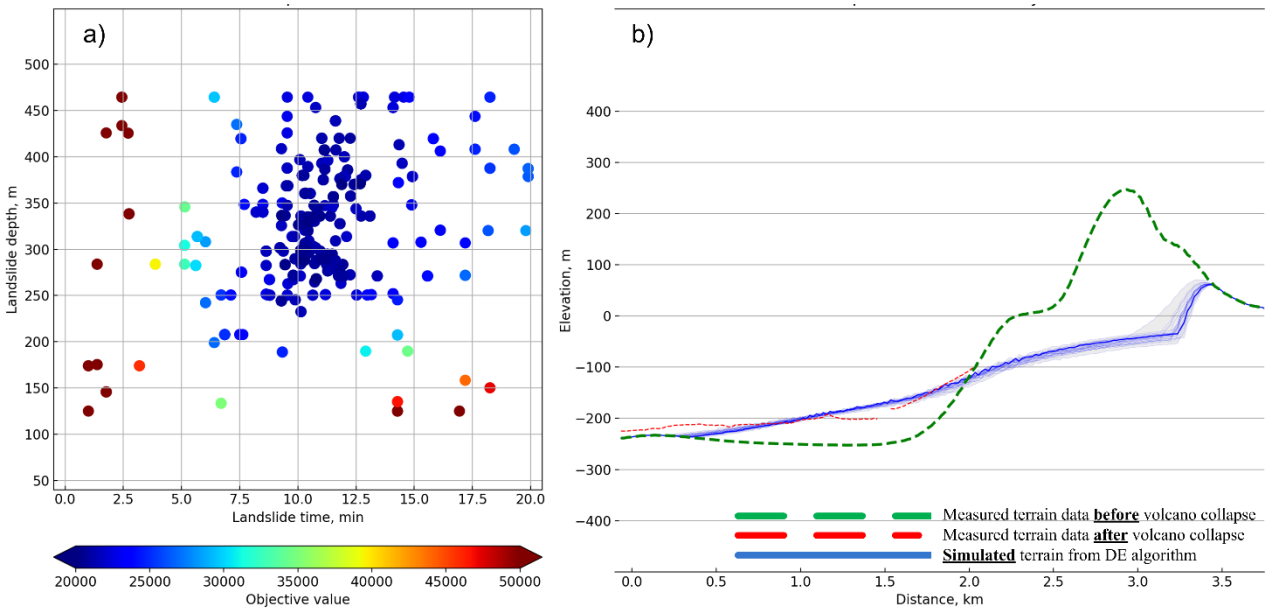

Fig. 6 – Global optimization results, a) the colored points give the value of the objective function for each simulation run, b) results of optimum parameter.

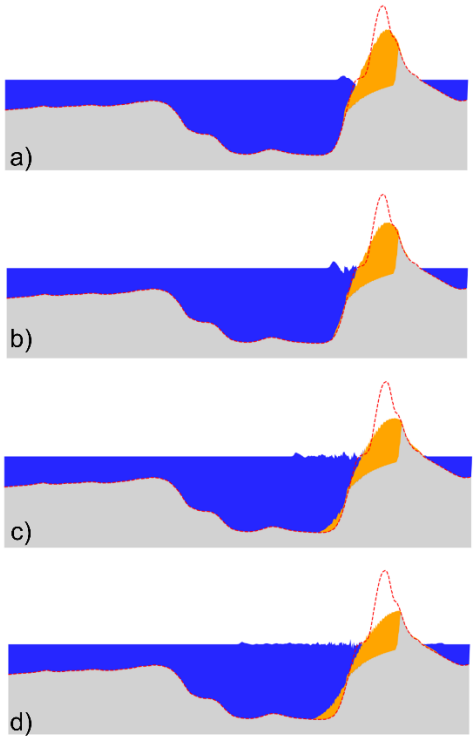

Fig. 7 – Temporal evolution of the tsunami wave from optimum landslide parameters after: a) 5 s; b) 10 s; c) 30 s; d) 60 s.

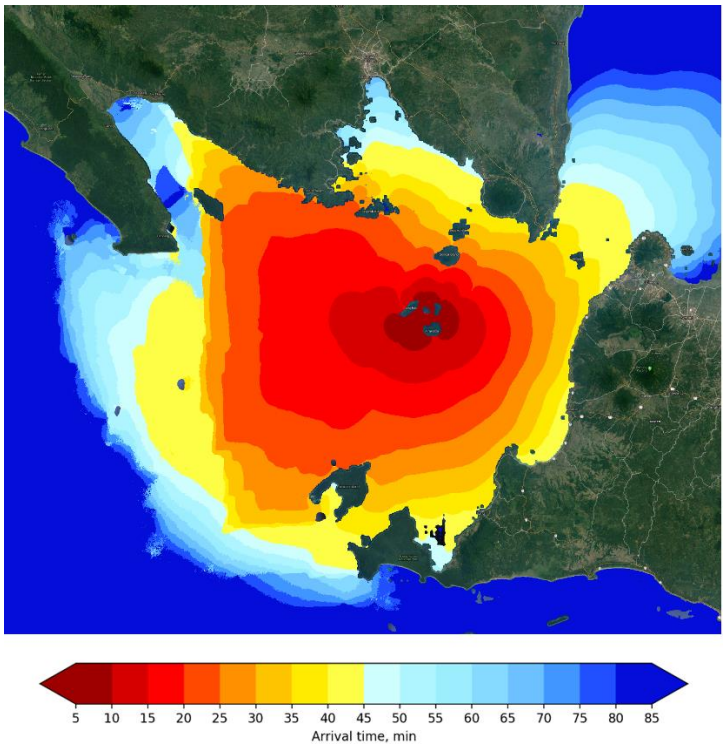

Fig. 8 – Arrival times of the leading tsunami wave measured by the positive amplitude when the wave amplitude is greater than + 0.3 m.

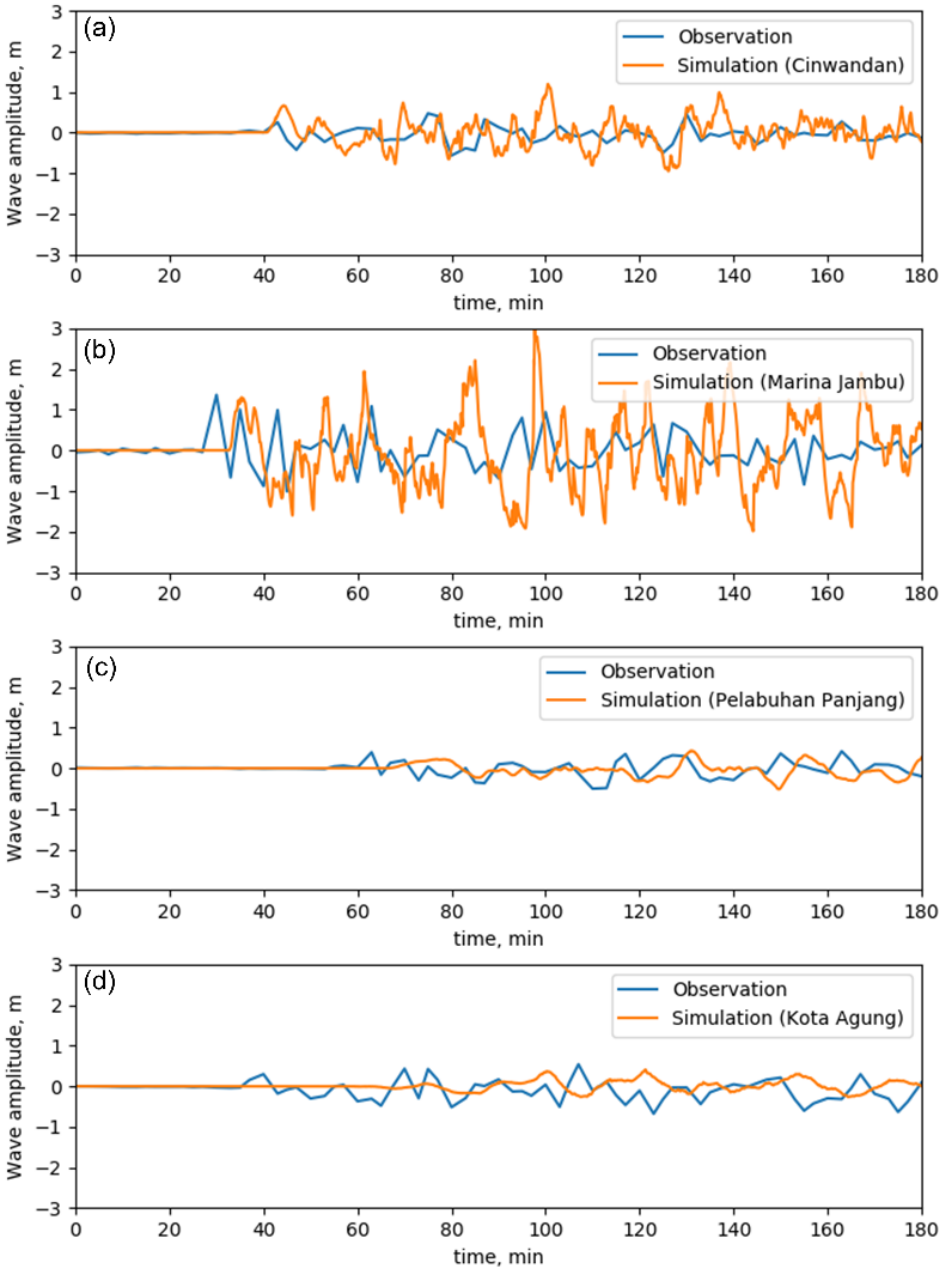

Fig. 9 – Comparison between observation and simulation at a) Ciwandan, b) Marina Jambu, c) Panjang, and d) Kota Agung.

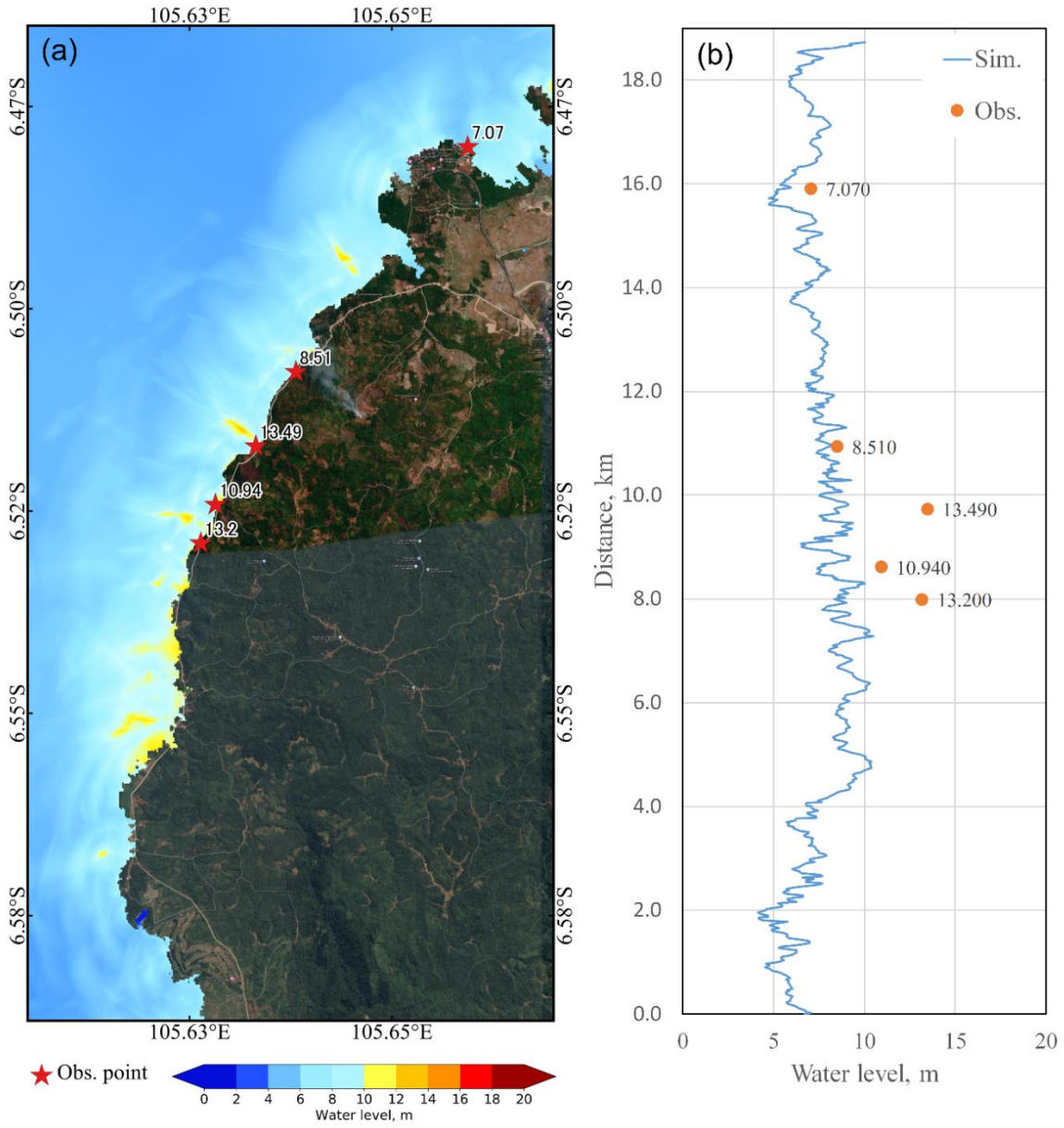

Fig. 10 – Impact of tsunami along the coastline in area D: a) flood extent and location of observation point; b) water level along the coastline and comparing to observation data.

The simulation snapshots of tsunami propagation at different times are shown in **Fig. 7** for 5, 10, 30, and 60 s after the tsunami was generated by the volcano eruption-induced landslide. Furthermore, a velocity decrease has been noted over the main high relief that produces an alteration in the concentric pattern in the arrival time map of the best fit parameters, as shown in **Fig. 8**. According to **Fig. 9**, which displays the tsunami wave amplitude time series at the tidal gauge around the Sunda Straits coast area with detided sea level. For the effects of the tsunami (from the best parameter), as shown in **Fig. 10**, along the coastline of Palu Bay are considered in the area D on **Fig. 1**. In the flood area on the coast, the observed tsunami height has an average value of approximately 10.5 m, with a maximum of 13.5 m at 10 km. A comparison of the simulation height with the surveyed sport presented in the underestimation as shown in **Fig. 10b**.

4. Conclusion

A large landslide was released from the south-western flank collapse of the Anak Krakatau volcano is modeled by a Two-layer model integrated code with a global optimization model to simulated the tsunami in the Sunda Straits. The parameter of the landslide model was estimated by the global optimization using the survey bathymetry after the event. The results show that the tsunami height of the best landslide parameter could reach up to 3-10 m along the shore on the underestimation to compare with the observation data. According to the wave form, the general wave pattern was well reproduced at the tide gauge during the event. Although the results are contained by some limitations. The landslide model was hypothesized by satellite images for the shape and the 3D ellipsoid for the volume. However, tsunami simulation related to this landslide is quite consistent with observed water heights.

Although there are many uncertainties in the tsunami hazard evaluation, such as submarine landslide geometry, bathymetric and topographic datasets, and numerical modeling, as mentioned above, the intention was not to perform a probabilistic hazard evaluation. Instead, this study proposes that a set of subaerial/submarine landslides could have produced the Sunda Straits tsunami triggered by the 2018 Anak Krakatau volcano eruption.

5. Acknowledgements

The observational data, tidal gauge records, were provided by the Coastal Disaster Mitigation Division, Ministry of Marine Affairs and Fisheries, Jakarta, Indonesia. This research was funded by the Willis Research Network (WRN) under the Pan-Asian/Oceanian tsunami risk modeling project and Pacific Consultants Co., LTD through the International Research Institute of Disaster Science (IRIDeS) at Tohoku University.

6. References

[1] Muhari A, Heidarzadeh M, Susmoro H, Nugrohh HD, Kriwati E, Suparto, Wijanarto AB, Imamura F, Arikawa T (2019): The December 2018 Anak Krakatau Volcano Tsunami as Intereed from Post-Tsuanmi Field Survays and Spectral Analysis. *Pure and Applied Geophysics*, **176** (12), 5219-5233.

[2] Syamsidik, Benazir, Luthfi M, Suppasri A, Comfort LK (2019): The 22 December 2018 Mount Anak Krakatau Volcanogenic Tsunami on Sunda Strait Coasts, Indonesia: tsunami and damage characteristics. Nat. Hazards Earth Syst. Sci. Discuss.

[3] Heinrich P, Boudon G, Komorowski JC, Sparks RSJ, Herd R, Voight B (2001): Numerical simulation of the December 1997 Debris Avalanche in Montserrat, Lesser Antilles. *Geophysical Research Letters*, **28**(13), 2529–2532.

[4] Shigihara Y, Goto D, Imamura F, Kitamura Y, Matsubara T, Takaoka K (2006): Hydraulic and numerical study on the generation of a subaqueous landslide-induced tsunami along the coast. *Natural Hazards*, **39**, 159–177.

[5] Kowalik Z, Murty TS (1993): *Numerical modeling of ocean dynamics* (p. 481). Singapore: World Scientific Pub.

[6] Satake K (1995): Linear and nonlinear computations of the 1992 Nicaragua earthquake tsunami. *Pure and Applied Geophysics*, **144**, 455–470.

[7] Heidarzadeh M, Krastel S, Yalciner AC (2014): The state-of-the-art numerical tools for modeling landslide tsunamis: A short review. In: Krastel S. et al. (eds), *Submarine Mass Movements and Their Consequences. Advances in Natural and Technological Hazards Research*, **37**, Chapter 43 (pp. 483–959). USA: Springer International publishing.

[8] Grilli ST, Harris JC, Tayebeh S, Bakhsh T, Masterlark TL, Kyriakopoulos C (2012): Numerical simulation of the 2011 Tohoku tsunami based on a new transient FEM co-seismic source: Comparison to far- and near-field observations. *Pure and Applied Geophysics*, **170**(6–8), 1333–1359.

[9] Titov VV, González FI (1997): *Implementation and testing of the method of splitting tsunami (MOST) model* (p. 11). NOAA Technical Memorandum ERL PMEL-112.

[10] Liu PLF, Woo SB, Cho YS (1998): *Computer programe for tsunami propagation and inundation.* Technical report; Cornell University: Ithaca, NY, USA.

[11] Imamura F, Imteaz MA (1995): Long waves in two-layers: Governing equations and numerical model. *Science of Tsunami Hazards*, **13**(1), 3–24.

[12] Lastras G, De Blasio FV, Canals M, Elverhøi A (2005): Conceptual and numerical modeling of the Big'95 debris flow, western Mediterranean Sea. *Journal of Sedimentary Research*, **75**, 784–797.

[13] Iglesias O, Lastras G, Canals M, Olabarrieta M, González M, Aniel-Quiroga I (2012): The BIG'95 submarine landslide-generated tsunami; a numerical simulation. *The Journal of Geology*, **120**(1), 31–48.

[14] Skvortsov A, (2002): *Numerical simulation of landslide generated tsunamis with application to the 1975 failure in Kitimat Arm, British Columbia, Canada*. PhD Thesis, School of Earth and Ocean Sciences, University of Victoria, British Columbia.

[15] Watts P, Grilli ST, Kirby JT, Fryer GJ, Tappin R (2003): Landslide tsunami case studies using a Boussinesq model and a fully nonlinear tsunami generation model. *Natural Hazards and Earth System Sciences*, **3**, 391–402.

[16] Fine I V, Rabinovich AB, Bornhold BD, Thomson RE, Kulikov EA (2005): The Grand Banks landslide-generated tsunami of November 18, 1929: Preliminary analysis and numerical modeling. *Marine Geology*, **215**(1D2), 45–57.

[17] Tinti S, Pagnoni G, Zaniboni F (2006): The landslides and tsunamis of the 30th of December 2002 in Stromboli analysed through numerical simulations. *Bulletin of Volcanology*, **68**(5), 462–479.

[18] Tinti S, Chiocci FL, Zaniboni F, Pagnoni G, de Alteriis G (2011): Numerical simulation of the tsunami generated by a past catastrophic landslide on the volcanic island of Ischia, Italy. *Marine Geophysical Research*, **32**, 287–297.

[19] Pakoksung P, Suppasri A, Imamura F, Athanasius C, Omang A, Muhari A (2019): Simulation of the Submarine Landslide Tsunami on 20 September 2018 in Palu Bay, Sulawesi Island, Indonesia, using a Two-Layer Model, *Pure and Applied Geophysics*, **176** (8), 3323.

[20] Grilli S, Tappin D, Carey S, Watt S, Ward S, Grilli A (2019): Modelling of the tsunami from the December 22, 2018 lateral collapse of Anak Krakatau volcano in the Sunda Straits, Indonesia. *Scientific Reports*, **9**, 11946.

[21] Ma G, Shi F, Kirby J (2012): Shock-capturing non-hydrostatic model for fully dispersive surface wave processes. *Ocean Modelling*, **43–44**, 22–35.

[22] Kirby J, Shi F, Nicolsky D, Misra S (2016): The 27 April 1975 Kitimat, British Columbia, submarine landslide tsunami: A comparison of modeling approaches. *Landslides*, **13**, 1421–1434.

[23] Shi F, Kirby J, Harris J, Geiman J, Grilli S (2012): A high-order adaptive time-stepping TVD solver for Boussinesq modeling of breaking waves and coastal inundation. *Ocean Modelling*, **43–44**, 36–51.

[24] Wang X, Liu PF (2006): An analysis of 2004 Sumatra earthquake fault plane mechanisms and Indian Ocean tsunami. *Journal of Hydraulic Research*, **44**, 147–154.

[25] Heidarzadeh M, Ishibe T, Sandanbata O, Muhari A, Wijanarto A (2020): Numerical modeling of the subaerial landslide source of the 22 December 2018 Anak Krakatoa volcanic tsunami Indonesia. *Ocean Engineering*, **20**, 195.

[26] Imamura F, Imteaz MA (1995): Long waves in two-layers: Governing equations and numerical model. *Science of Tsunami Hazards*, **13**(1), 3–24.

[27] Macías J, Vázquez JT, Fernández-Salas LM, González-Vida JM, Bárcenas P, Castro MJ (2015): The Al-Borani submarine landslide and associated tsunami. A modelling approach. *Marine Geology*, **361**, 79–95.

[28] Storn R, and Price K (1997): Differential evolution—A simple and efficient heuristic for global optimization over continuous spaces, *J. Global Optimization*. **11**, 341– 359.

[29] Gylfadottir SS, Kim J, Helgason JK, Brynjolfsson S, Hoskuldsson A, Johannesson T, Harbitz CB, Løvholt F (2017): The 2014 Lake Askja rockslide-induced tsunami: Optimization of numerical tsunami model using observed data, *J. Geophys. Res. Oceans*. **122**, 4110– 4122.

